HHS Public Access

Author manuscript

Nat Biotechnol. Author manuscript; available in PMC 2020 May 22.

Published in final edited form as:

Nat Biotechnol. 2019 September ; 37(9): 1013–1023. doi:10.1038/s41587-019-0198-8.

Next-generation interfaces for studying neural function

James A. Frank[1,2], **Marc-Joseph Antonini**[1,2,3], **Polina Anikeeva**[1,2,4,*]

[1]Research Laboratory of Electronics, Massachusetts Institute of Technology, Cambridge, MA, USA.

[2]McGovern Institute for Brain Research, Massachusetts Institute of Technology, Cambridge, MA, USA.

[3]Harvard/MIT Health Science & Technology Graduate Program, Cambridge MA, USA

[4]Department of Material Science and Engineering, Massachusetts Institute of Technology, Cambridge, MA, USA.

Abstract

Monitoring and modulating the diversity of signals used by neurons and glia in a closed- loop fashion is necessary to establish causative links between biochemical processes within the nervous system and observed behaviours. As developments in neural interface hardware strive to keep pace with rapid progress in genetically encoded and synthetic reporters/modulators of neural activity, the integration of multiple functional features becomes a key requirement and a pressing challenge in the field of neural engineering. Electrical, optical, and chemical approaches have been used to manipulate and record neuronal activity *in vivo*, with a recent focus on technologies that both integrate multiple modes of interaction with neurons into a single device and enable bidirectional communication with neural circuits with enhanced spatiotemporal precision. These technologies are not only facilitating a greater understanding of the brain, spinal cord and peripheral circuits in the context of health and disease, but also informing the development of future closed-loop therapies for neurological, neuro-immune and neuroendocrine conditions.

The human nervous system is composed of a heterogeneous network of cells that communicate with each other through electrical, chemical, and physical signals. Diseases of the nervous system, including Alzheimer's, Parkinson's and epilepsy, affect >100 million people and represent a >$800 billion annual burden in the United States alone[1]. Treatments for these disorders often rely on pharmacotherapy or implanted electrical stimulation devices, but they are generally not specific to neuronal subtypes and thus are accompanied by side effects. This arises as a result of our poor understanding of the underlying mechanisms of action of these interventions, alongside a lack of available tools to interact with the brain at meaningful levels of precision and depth. To fully appreciate this

*Correspondence should be addressed to P.A (anikeeva@mit.edu).

Author contributions

J.A.F. and M.-J.A. researched data for the article. J.A.F. M.-J.A. and P.A. discussed the article scope and wrote the manuscript.

Competing interests

The authors declare no competing interests.

complexity, new probes must be developed to deliver and record signals through multiple modalities, while minimizing unwanted side-effects[2].

In this review, we discuss principles that should be considered when designing next-generation neural interfaces to communicate bi-directionally with neural circuits through multiple modalities. Advances beyond classic electrical stimulation and recording techniques will likely contribute to understanding and treating disorders of the nervous system. These efforts will help link the physiological processes associated with neuronal function to normal and pathological behaviour as well as enabling closed-loop bio-interfaces for therapeutic intervention.

Integration challenges in a multimodal neural interface

To understand neurological disorders and the mechanisms that drive behaviour, we must interrogate neural circuits spanning areas across the brain (Fig. 1a). Conversely, each neuron has thousands of synaptic connections that are uniquely regulated by a palette of receptors that vary at the subcellular level (Fig. 1b–d). Neurotransmission also varies dramatically in temporal resolution, from the sub-microsecond span of action potential firing to hour-long fluctuations in hormone concentrations or gene expression (Fig. 1e). Signalling events are heavily compounded and their strength can vary by orders of magnitude; for example, neurotransmitter secretion, which occurs at concentrations ranging from pM (10^{-12}M) to μM (10^{-3} M) (ref. 3).

Consequently, when designing neural interfaces, one must consider a multitude of factors, including: spatial resolution, temporal precision, sensitivity and the cellular selectivity with which signals can be delivered or recorded. Neurotransmission is multimodal in nature, thus the devices themselves should possess multiplexed capabilities and the physical properties of the implanted hardware should be carefully engineered (Table 1). Size and flexibility must also be considered, as the mechanical mismatch between stiff implanted devices (1–100 GPa) and the soft brain tissue (kPa–MPa) can yield tissue damage and elicit a foreign body response that eventually blocks the interface through glial scarring. With these characteristics in mind, developments in materials, manufacturing techniques and signalling modalities will open doors to new experimental techniques and further understanding of neural processes.

Electrical recording and stimulation of neural activity

Since the first electroencephalography (EEG) recording in 1938 (ref. 11), numerous neural implants to stimulate and record electrical activity in the brain have been developed. Advanced fabrication techniques made available by the electronics industry have delivered silicon (Si)-based Utah arrays and Michigan probes[3,4] (Fig. 2a,b) and have enabled the extreme miniaturization and dense packing of electrodes in the Neuropixel[5]. Integrated with a complimentary metal-oxide-semiconductor (CMOS) platform, the Neuropixel offers 960 recording sites along 10 mm long shanks with a 70×20 μm^2 cross section and can record well-isolated action potentials from hundreds of neurons (Fig. 2c).

As the mechanical and chemical mismatch between probes composed of hard materials (including metals, glasses, and semiconductors) often yields a foreign-body response and gliosis in neighbouring tissue[6,7], soft materials are increasingly being adopted in neural interfaces to minimize these effects. A notable example, the Neural Mesh, comprises 16 platinum (Pt) recording or stimulating electrodes (20 μm and 150 μm in diameter, respectively) deposited onto gold (Au) interconnects sandwiched by layers of a photoresist SU-8 (20 μm width and ~400 nm thick). The open architecture allows these probes to integrate with the brain tissue following injection via a needle[8] (Fig. 2d). The Neural Mesh permits recording of local field potentials and single-unit action potentials; it can deliver electrical stimulation over 8 months in the mouse brain. In a follow-up study, this platform was adapted to record single-unit activity from the retina of awake mice[9]. Mesh-based electrode arrays composed of porous and transparent graphene[10], or composite/metal nanowires[11] deposited on flexible and stretchable substrates, have been applied as conformal cortical surface probes and stimulation electrodes (Fig. 2e,f). These devices take the shape of the surface to which they are applied, and this approach has also been used to prepare spinal[12] and cardiac interfaces.[13]

Organic conductors have been explored vigorously in recording and stimulation electrodes due to their promising mechanical and electrochemical interfaces with the neural tissue[14]. Because of its biochemical stability and ability to form both electronic and ionic interfaces with the cells in physiological fluids, the organic semiconductor poly(3,4-ethylenedioxythiophene):poly(styrenesulfonate) (PEDOT:PSS) and its chemical derivatives are often exploited in coatings to reduce the impedance and increase the charge injection capacity (CIC) in miniaturized electrodes. For example, 8.4 μm carbon fiber microelectrodes have been coated with PEDOT:poly(toluenesulfonate) (PEDOT:PTS) to lower the tip impedance from 6.8 MΩ to ~120 kΩ at 1 kHz[15]. This array is capable of recording single unit action potentials from the rat motor cortex for 3 months, inducing only negligible glial scarring[16]. Another system, the Neurogrid[17], employed PEDOT:PSS as a gate in organic electrochemical transistors on a 4 μm parylene C structure. This permitted recording of isolated action potentials from the cortical surface with high signal-to-noise ratio (SNR). A systematic study has recently quantified electronic and ionic transport between PEDOT-based electrodes and physiological environments, informing design of interfaces for optimized SNR and CIC[18].

The transition of high-resolution, low-modulus electrodes with improved impedance and CIC to the clinic will likely provide spatiotemporally precise alternatives to the millimetre-thick clinical deep brain stimulation electrodes. When paired with artefact rejection circuits and algorithms to permit simultaneous stimulation and recording[19], these electrodes will also empower closed-loop therapeutic neuromodulation. Furthermore, integration of electrophysiology and electrical stimulation with the chemical and optical neural interrogation approaches will undoubtedly facilitate fundamental studies of neuronal dynamics and inform the abovementioned clinical interventions.

Light-controlled stimulation or silencing of neuronal activity using opsins.

Genetically cells or circuits can be manipulated with sub-microsecond precision through incorporation of light-sensitive proteins—the rapidly evolving field of optogenetics[2,20]. The blue-light sensitive cation channel channelrhodopsin 2 (ChR2), which depolarizes cells on activation, remains the workhorse tool for neural excitation[21], despite its early introduction to neuroscience (more than a decade ago; Fig. 3a). Thousands of studies have leveraged ChR2 to dissect the roles of specific brain regions, neuronal types, and projection circuits in controlling behaviours spanning motivation, movement, circadian rhythm, addiction, anxiety, memory, aggression and social interactions, among others[22–25]. Over the past decade, ChR variants with red-shifted activation spectra[26], modified kinetics[27], or subcellular localization[28] have also been developed to expand our stimulation capabilities.

Complementary to neural excitation with photosensitive cation channels, inhibition is achieved with opsins that hyperpolarize the membrane. Inhibitory opsins, such as proton (H^+)[29] or sodium (Na^+)[30] pumps, as well as chloride (Cl^-)[31,32] channels, have been engineered for enhanced sensitivity and modified activation spectra and kinetics (Fig. 3b). For example, the blue light-activated H^+-pump Arch3 silences neurotransmission by increasing cellular pH[29]. When fused to a pH-sensitive green fluorescent protein (GFP) and targeted to synaptic vesicles or lysosomes, the Arch-based pH probe pHeonix can control intracellular organelle acidification and provide an optical readout[33]. Moreover, rhodopsin-linked enzymes allow optical control of second messenger metabolism, such as the rhodopsin-guanylyl cyclase CaRhGC and rhodopsin-adenylyl cyclase CaRhAC, which on green irradiation generate cGMP or cAMP, respectively[34] (Fig. 3c).

As the use of optogenetic tools in neuroscience continues to expand, so does the demand for probes capable of simultaneous optical modulation and monitoring of neural activity. Although commercially available silica fibers remain a staple of optogenetic studies, advanced probes, such as tapered optical fibers, allow stimulation of multiple spatially restricted brain regions using different wavelengths[35]. Moreover, the burgeoning interest from the neural engineering community has delivered a diversity of integrated optoelectronic probes, including Michigan-style[36] and Utah-style arrays[37] with monolithically integrated light-emitting devices (LEDs), microcontact printed flexible probes equipped with microscale LEDs (μLEDs)[38], arrays of transparent conductive nanopillars[39], and multifunctional polymer-based fibers[12,40,41]. These platforms have been extensively reviewed elsewhere[42], and in the later sections, we discuss these emerging tools with expanded capabilities that further empower optogenetic studies.

Light-controlled neural signalling using LOV domains and cryptochromes.

Besides opsins, other optogenetic motifs can be used to engineer light-responsive proteins to control enzymatic activity or gene expression through protein sequestration, rearrangement, fragment condensation, or translocation[43]. The LOV (light oxygen voltage)-domain can regulate activity or protein access through conformational rearrangements induced by blue irradiation. In the FLARE (fast light- and activity-regulated expression)[44] and Cal-Light approaches[45], a transcription factor is tethered to the membrane via a linker containing a

calmodulin-binding motif and a protease cleavage site that is sterically blocked by the dark-state LOV-domain. During neuronal activation, increased intracellular calcium ion (Ca^{2+}) concentration recruits or reconstitutes a calmodulin-linked protease in proximity to the membrane linker. LOV-domain photoactivation unmasks the cleavage site to release the transcription factor from the plasma membrane, driving gene expression (Fig. 3d). These optogenetic coincidence detectors can be applied to express opsins with activity-dependent cellular resolution, and specific neurons can later be activated or inhibited to confirm their role in behaviour.

Optogenetic dimerizers (e.g., the cryptochrome-based CRY2-CIB heterodimerization motif) can on irradiation with blue light, fuse split-enzymes or control protein translocation[46]. The CIB domain can be genetically targeted to specific subcellular locations, and fusion of CRY2 to a target protein can control its localization on demand. This was used to generate an optogenetic cAMP-dependent protein kinase (optoPKA)[47], which could be reversibly activated on the mitochondria, cytoskeleton or plasma membrane (Fig. 3e). The emerging diversity of light-sensitive biological machinery will enable rational design of optogenetic tools to manipulate and probe molecular mechanisms of neurotransmission *in vivo* with the goal of correlating these molecular processes to behaviour in the context of health and disease.

Genetically encoded fluorescent reporters to monitor neural activity

Fluorescent reporters for ions or small molecules enable monitoring of neural activity from the subcellular to population scales[48]. Genetically encoded Ca^{2+} indicators (GECIs) remain the gold standard for imaging neural activity (Fig. 3f), and they enable entire cortical circuits to be monitored in awake head-fixed mice using wide-field and two-photon imaging[49]. In addition to green-emitting GCaMPs[50] (GCaMP is a fusion of circularly permutated GFP, calmodulin, and M13 peptide sequence from myosin light-chain kinase), red-shifted GECIs allow imaging in deeper tissues and can be used for multiplexed recording from orthogonal cell populations[51]. Similarly, genetically encoded voltage indicators (GEVIs) can record action potentials over large tissue volumes with sub-microsecond resolution. Closed-loop robotic directed evolution was used to engineer Archon1 for improved brightness and membrane localization[52]. In the ‘Floxopatch’ mouse line, the near-infrared opsin-based GEVI QuasAr2 (Fig. 3g) and the blue-shifted cation channel CheRiff are expressed in a Cre-dependent manner[53]. This allows dual-color stimulation/recording in genetically defined cell populations. Other biomolecules or neurotransmitters can be imaged using encodable optical biosensors[54,55]. Probes for glutamate (SF-iGluSnFR)[56], dopamine (dLight1[57] and $GRAB_{DA}$[58]) acetylcholine (GACh)[59] or glycine (GlyFS)[60] enable real-time imaging of neurotransmitter release via one- or two-photon imaging. Expansion of this approach to other signalling molecules in combination with new probe hardware, sensors, and multi-color imaging will allow dissection of the temporal dynamics of neurotransmitter and biomarker release, reuptake, and ion flux.

Although conventional fluorescence microscopy enables recording of neural activity at multiple scales, it remains mostly limited to applications in head-fixed subjects. Implantable endoscopes based on gradient index (GRIN) optics[61] and solid-state detectors (e.g.,

Miniscope[62]) permit activity-dependent imaging in the brain of moving rodents. Although the former are available commercially, the latter can be assembled from off-the-shelf parts using open-source instructions. Although fluorescence endoscopy of subcortical structures using the Miniscope requires removal of the cortical tissue, combining this method with two-photon excitation affords less invasive access to deeper brain areas[63].

Fiber photometry uses an implanted fiber optic to both excite and collect the emission from GECIs to record activity from populations of neurons (Fig. 3h)[64]. Although spatial resolution is limited by the size of the fiber core and the scattering properties of the neural tissue, genetic targeting allows monitoring of specified neurons in freely moving subjects. Up to 7 spatially distinct brain regions can be simultaneously monitored in behaving animals using frame-projected independent-fiber photometry (Fig. 3i)[65], where signals from a bundled fiber are integrated by a CMOS camera. When applied to GEVIs, the TEMPO (trans-membrane electrical measurements performed optically) approach[66] can record local field potentials from defined cell populations without physiological noise fluctuations. Application of fiber photometry to other fluorescent biosensors will be instrumental in determining how neurotransmitters fluctuate in deep brain regions of behaving subjects. Notably, a multimode fibre-based endoscope permits the imaging of fluorescent proteins within deep brain regions[67]. Although it has yet to be applied to reporters of neural activity, this device may increase the applicability of fiber photometry to monitor neural activity in deep brain regions with cellular resolution.

In addition to implantable optical probes that rely on external optoelectronics for signal detection, micro-contact printing techniques have recently permitted direct integration of μLEDs and photodetectors[68] (Fig. 3j). Such optoelectronic probes allow illumination and detection of reporter fluorescence at the point of implantation. This eliminates the need for collection optics and fiber tethers and is compatible with wireless data and power transfer.

Electrical and microfluidic detection of neurotransmitters and biomarkers.

Although signals propagate along the neuronal membrane in the form of an electrical potential wave, transmission between neurons happens at the synaptic cleft via release, reuptake, and metabolism of neurotransmitters[69]. Understanding spatiotemporal dynamics of chemical neurotransmission will allow dissection of the molecular mechanisms underlying many neurological disorders[70]. Electroactive biogenic amines, such as dopamine, norepinephrine, serotonin and histamine, can be detected in real-time using *in vivo* fast scan cyclic voltammetry (FSCV). This approach relies on rapid potential sweeps at implanted electrodes to oxidize and reduce nearby analyte molecules, and the voltammogram shape offers information about the target analyte[70,71] (Fig. 4a). FSCV excels in temporal resolution (<100 ms) and sensitivity, but remains limited in terms of its selectivity. Chemically similar electroactive species (e.g., dopamine and norepinephrine) can complicate the analysis, but principal component analysis (PCA) may be used to deconvolute signals from distinct neurotransmitters[72,73].

Despite decades of research, the majority of FSCV experiments are still conducted with probes composed of a single carbon fiber microelectrode housed in a glass capillary[74] (Fig. 4b). These probes have been applied to chronic long-term monitoring of dopamine dynamics

in primates[75] and mice[76]. Moreover, simultaneous voltammetric detection of dopamine and oxygen can be combined with single-unit electrophysiological recordings to demonstrate fluctuations in these biomarkers correlated with widespread electrical activity following brain injury[77]. Notably, FSCV is compatible with optical stimulation using ChRs[78], and the development of more advanced probes with improved optical capabilities will allow FSCV to be used in conjunction with optical reporters to simultaneously monitor both electroactive and non-electroactive species with high temporal resolution.

Functional coatings can be deposited to improve electrode stability, sensitivity and analyte selectivity. Coating a tungsten electrode with a boron-doped diamond film afforded an FSCV probe with improved mechanical and electrochemical stability[79]. Sensitivity was enhanced by increasing the electrochemical interface area and improving surface adsorption, as was demonstrated with electrodeposited PEDOT-graphene oxide (PEDOT-GO) coatings[80]. When compared with uncoated carbon electrodes, PEDOT-GO increases dopamine detection sensitivity by 880% and reduces the limit of detection by 50% (to ≈20 nM). Analyte selectivity can be enhanced by integrated size-exclusion membrane coatings for detection of low molecular weight molecules like hydrogen peroxide[81]. Moreover, enzyme-coated electrodes widen the scope of accessible analytes, and allow detection of non-electroactive biomarkers, such as glucose[82,83], and could be further expanded to detect lactate[84], choline and acetylcholine[85], and glutamate[86].

As a complement to voltammetry, microdialysis allows quantification of a vast array of biomarkers within the sampled fluid, independent of their electrochemical activity. Typical microdialysis probes consist of inlet and outlet capillaries within a hollow-fiber that is sealed by a semi-permeable membrane and infused with buffer[87] (Fig. 4c). The collected analytes are subject to chemical analytics including high performance liquid chromatography and mass spectrometry[88], and sample derivatization permits detection of up to 70 analyte molecules from a single sample[89]. Microdialysis thus provides exquisite chemical resolution and a wide sensitivity range towards diverse analyte molecules[69], but the low sampling rate (often >10 min) and offline analysis limit its temporal resolution in real-time applications. The slow sampling rate also limits the spatial resolution, as diffusion of analytes through the tissue is a major factor at these timescales. Continuous online microdialysis (coMD)[90] is being used in clinic for diagnosing and monitoring traumatic brain injury[91]. The coMD approach uses ion-selective electrodes and dedicated sensors to perform real-time recording of multiple ions (K^+) and small molecules (e.g., glucose and lactate). It can also complement electrocorticography (ECoG) recordings to understand how these biomarkers fluctuate with neural activity.

Microdialysis probes often exceed 200 μm in diameter[92]; thus, a microfabricated Si-based probe with 45×180 μm^2 dimensions increases the spatial resolution and reduces the surrounding tissue damage[93] (Fig. 4d). This microfabricated Si-based probe possesses an etched U-shaped channel and a nanoporous membrane along the tip and can quantify amphetamine-stimulated dopamine release in the rat striatum with accuracy comparable to a standard dialysis probe. Similar to FSCV, microdialysis is also compatible with optical tools. A hybrid device composed of a light-guide embedded within a microdialysis probe has also been used to measure extracellular dopamine and glutamate in response to optogenetic

stimulation within the mouse brain[94]. In a more recent example, an opto-dialysis probe was able to monitor optically evoked release of multiple opioid peptides alongside dopamine, gamma aminobutyric acid (GABA), and glutamate in freely moving mice[95]. Future integration of more advanced microfluidic probes with optical capabilities will allow real-time imaging of neural activity concomitant with biomarker analysis with increased spatiotemporal precision.

Chemical approaches for stimulating neural cells

Chemical probes can address the roles of specific receptors and downstream pathways on cell physiology. Designer receptors exclusively activated by designer drugs (DREADDs) are chemogenetic tools based on G protein-coupled receptors (GPCRs) engineered to respond exclusively to an otherwise inert ligand[96,97]. DREADDs retain the natural downstream signalling properties of their parent receptor, allowing activation and inhibition of target neurons on systemic addition of the exogenous ligand. However, this approach offers limited spatial resolution and temporal precision restricted by slow on/off kinetics. For targeting endogenous receptors with increased precision, light-responsive molecules can transmit an optical stimulus into a cellular response. Caged ligands, the activities of which are masked by a photo-labile protecting group, become irreversibly activated on illumination (Fig. 5a). Alternatively, permanent attachment of a photoswitch to a drug molecule can afford *reversible* optical control of the target[98], and a variety of ions/neurotransmitters and their receptors have therefore been placed under optical control[99]. Synthetic tuning of the photo-cages or switches permits activation/inactivation with far-red or two-photon irradiation[100,101] and can even target ligands to subcellular compartments[102,103].

Self-labelling enzyme tags covalently tether molecular probes to defined locations with subcellular accuracy[104]. These include SNAP (an O6-alkylguanine-DNA-alkyltransferase that reacts with O6-benzylguanine derivatives), CLIP (an O2-alkylcytosine-DNA-alkyltransferase that reacts with O2-benzylcytosine derivatives) or Halo-tag (a haloalkane dehalogenase that reacts irreversibly with primary alkylhalides)—enzymes that react with a functional group at one end of the linker to tether the pharmacophore to the target. For example, the DART (drugs acutely restricted by tethering) approach uses the Halo-tag to target an α-amino-3-hydroxy-5-methyl-4-isoxazolepropionic acid (AMPA)-receptor agonist to either striatal dopamine 1 (D1) or D2 receptor-expressing cells in a Parkinson's mouse model[105]. Similarly, optical control of a SNAP-metabotropic glutamate receptor 2 (mGluR2) receptors in retinal ganglion cells using a BGAG (SNAP-reactive benzylguaninie (BG) at one end, a linker, and an azobenzene-glutamate (AG) at the other end)-tethered photoswitchable glutamate restores light-responses in the blind mouse retina *in vivo*, enabling patterned vision[106] (Fig. 5b).

Importantly, multiplexed stimulation of distinct cell populations or receptor subtypes can be achieved through selective expression of orthogonal enzyme tags[107]. Antibodies can also be used to target molecules to defined locations. In the chromophore-assisted light inactivation (CALI) approach (Fig. 5c)[108], an antibody-conjugated photosensitizer could selectively inactivate target receptors through localized generation of singlet oxygen. This has been used to inactivate AMPA receptors in the mouse hippocampus, and to erase fear memory *in*

vivo during behaviour. Future synthetic efforts will expand these approaches to other ligands/receptors, and implantable devices that permit simultaneous viral and chemical delivery alongside optical stimulation will facilitate the use of these technologies in freely moving animals.

Synthetic and semi-synthetic probes for molecule and ion detection

Small-molecule ion- or voltage-sensitive dyes allow imaging of neural activity without the need for genetic manipulation, and their selectivity/sensitivity can be systematically tuned through chemical modification. For example, the red-shifted Ca^{2+} sensor Cal-590 permits *in vivo* two-photon imaging up to 1 mm deep within the mouse cortex[109]. It can be applied by extracellular perfusion, or localized to single cells by electroporation through a patch pipette. Rhodamine-based voltage dyes (RhoVRs) possess increased dynamic range, permit visualization of single action potentials in deep tissues[110], and can be used in conjunction with green-emitting Ca^{2+} indicators for multiplexed imaging.

Semi-synthetic biosensors possess the advantage of genetic targetability while retaining the synthetic malleability of small-molecule dyes. Tethering hydrogen-sensitive dyes to the inside to synaptic vesicles using SNAP-tags allows visualization of exocytosis and endocytosis in hippocampal neurons[111]. An alternative strategy for measuring NAD^+ or NADPH/$NADP^+$ levels (NAD-Snifit and NADP-Snifit, respectively) employs orthogonal bioconjugation (SNAP- and Halo-tags) to tether a Förster resonance energy transfer (FRET) fluorophore-pair to defined locations on a ligand binding domain[112]. FRET changes induced on analyte binding allow NAD(P) levels to be quantified in real-time (Fig. 5d). These hybrid probes can be applied to a wide array of analyte molecules and used *in vivo* alongside the development of the appropriate hardware.

Approaches for small molecule and gene delivery

Achieving the delivery of small molecules *in vivo* with precision comparable to chemical neurotransmission remains a challenge. Local injections bypass the blood-brain-barrier and generate high local drug concentrations while reducing the potential for off-target effects associated with systemic injections. Although conventional cannulas are still commonly used, microfabricated probes with enhanced capabilities and improved biocompatibility have emerged. For instance, the Chemtrode integrates a microfluidic channel with a microelectrode array, enabling injection of up to three different drugs alongside simultaneous electrophysiology at 7 recording sites[113] (Fig. 5e). The microfluidic ion pump, μFIP, uses electrophoresis to drive solvent-free delivery of ions, such as K^+ and $GABA^-$, across a membrane to the target region[114].

Controlling gene delivery across different scales is vital to understand the roles of individual cells, or interface with large functional areas of the brain (Fig. 5f). Single-cell transduction can be achieved using the virus-stamping approach[115], where viral particles are reversibly bound to the surface of iron nanoparticles placed in a micropipette solution. The micropipette is inserted into the brain and positioned against the target cell, and magnetic field application directs the particles to the target cell surface. This technique is compatible

with several viruses commonly used in optogenetics and can be exploited to transduce other biosensors into single cells. Conversely, large functional areas can be transduced by functional coatings of silk fibroin mixed with AAV capsids (Fig. 5g). When applied to the surface of implants, such as optical fibers or cranial windows[116], this approach ensures widespread virus expression at the site of the implant and simplifies the surgical implantation procedure. Alternatively, engineered viral capsids that can cross the blood brain barrier, such as AAV- PHP.eB, allow widespread, non-invasive labelling throughout the entire CNS following systemic injection[117]. These approaches will be especially useful when applied to optogenetic probes or biosensors for expression in large mammals.

Multi-modal interaction with cells and tissues

To keep pace with the ever expanding palette of molecular and genetic tools for controlling and recording neural activity, emerging neural interfaces must integrate multiple functional features to deliver electrical, optical, and chemical signals to and from the neural tissue. Such probes will enable bi-directional communication with the neural circuits and accelerate fundamental studies of their physiological and pathological outputs.

The most straightforward approach to integrate multiple functionalities is to fuse disparate existing technologies. For example, addition of a nanoelectronic coating to the surface of a device (e.g., a silica optical fiber or a micropipette) endows it with electrical recording capabilities for delivering a bi-modal probe (Fig. 6a)[118]. Alternatively, a miniaturized neural drug delivery system (MiNDS) has been reported relying on a tungsten recording electrode and two microfluidic channels housed in a stainless steel needle[119] (Fig. 6b). This device has been used to record and chemically stimulate deep brain regions in non-human primates. The fusion of soft microfluidic channels to an integrated array of inorganic μ-LEDs (μ-iLEDs) on a flexible substrate has also been used to create an optofluidic system that delivers not only drugs and viruses to the brains of freely moving rodents, but also concurrently confers the ability to photostimulate neural activity[120] (Fig. 6c). Although this approach enables the design of multifunctional devices, it is often limited by the device footprint, which increases with the addition of each new functionality.

Leveraging well-established micro- and nano-fabrication techniques permits scalable production of miniaturized devices with densely packed features. For example, optoelectronic integration has been applied to produce a multi-shank optoelectrode that allows dual-color photostimulation and electrical recording at multiple sites (Fig. 6d)[121,122]. Each silicon shank integrates two laser diodes and iridium electrodes allowing recordings alongside dual-color photostimulation *in vivo*. Similarly, using polydimethylsiloxane (PDMS) as a substrate, the electronic dura matter integrates microfluidic channels with recording and stimulating electrodes onto a flexible, transparent and stretchable probe, which has been used to restore locomotion after spinal cord injury in rodents[123]. Microfabrication techniques have also been employed to prepare a T-junction low-flow, push-pull microdialysis probe, which additionally houses platinum electrodes capable of electrical stimulation and recording (Fig. 6e)[124].

The use of transparent substrates and electrodes can endow electrophysiological probes with optical capabilities without increasing their footprint. The deposition of transparent electrode arrays onto polymer substrates permits simultaneous electrical recording and optogenetic stimulation[125] or fluorescent imaging with GECI[126] on the cortical surface (Fig. 6f). Two-photon imaging and optogenetic excitation extends these approaches to deeper tissues[127,128]. In another approach, silicon-based biointerfaces leverage the photoelectric, photoacoustic, and photothermal properties of silicon to stimulate neurons through multiple modalities. These can be shaped into nanowires, flat nanomembranes or flexible mesh arrays to generate thermal, faradaic or mechanical signals upon irradiation[129]. These interfaces can also be tailored to allow intercellular, intracellular, and extracellular optical control of neural activity without the need for genetic modification.

An alternative strategy to enable multifunctional integration at the microscale, employed by our laboratory, is to apply thermal drawing of multi-material fibers offers (Fig. 6g)[41]. Fibers combining optical neuromodulation, microfluidic delivery of drugs and viruses, and electrophysiological recording capabilities can be produced in kilometer lengths from macroscale models by application of heat and tension. These devices have recently enabled monitoring of opsin expression in cell bodies and axonal terminals, informing projection mapping in behavioural studies[40,130]. Moreover, application of fiber drawing to elastomers has delivered stretchable probes suitable for chronic recording and optogenetic neuromodulation in the rodent spinal cord[12]. Going forward, innovations in materials chemistry and thermal drawing techniques are anticipated to expand the sensing and modulation capabilities of fiber probes, while maintaining their miniature and flexible form factors.[131–133]

Conclusions and perspective

The nervous system is formed by a vast network of cells communicating through a plethora of stimuli. To fully appreciate this complexity, next-generation technologies must communicate with the neural tissue bi-directionally through a variety of modalities, time-scales, and sensitivities, while spanning the nanometre to centimetre scales. Fabrication techniques and materials must evolve accordingly to accommodate novel optical and chemical probes to facilitate their use in behaving subjects, while offering the ability to continuously record multiple biomarkers. Importantly, alongside this ever-expanding toolkit of neural probes comes increasing experimental complexity that can impede data interpretation. Certain modalities are not compatible when applied simultaneously in spatially restricted areas of the brain, and can cause confounding artefacts that skew experimental observations. As such, great care must be taken when selecting tools for each experiment, and appropriate control experiments must be performed to avoid unsupported or erroneous conclusions. However, when used correctly these tools will enable studies of the molecular mechanisms underlying behavioural and physiological phenotypes and facilitate integration of molecular and systems neuroscience. The insights delivered by such integrated studies will inform therapeutic approaches for neurological and psychiatric conditions with heterogeneous pathophysiology and temporally evolving signatures.

Although most tool development thus far has focused on interrogation of neurons, glia are emerging as increasingly important players in the functioning nervous system, and approaches to exclusively target glial biology and signalling are urgently needed. Applications to other electroactive tissues present entirely different challenges, such as cell-type diversity, different time-scales for activation, and different sets of chemical and physical signals[134]. This provides biologists and engineers with endless research opportunities, and the urgency to develop therapeutic interventions for disorders of the aging nervous system should motivate the translation of these emergent approaches and insights from the lab and into the clinic.

Acknowledgements

This work was supported in part by the National Institute of Neurological Disorders and Stroke (5R01NS086804), by the National Institutes of Health BRAIN Initiative (1R01MH111872), by the National Science Foundation through the Center for Materials Science and Engineering (DMR-1419807) and the Center for Neurotechnology (EEC-1028725), and by the McGovern Institute for Brain Research at MIT.

References

1. Gooch CL, Pracht E & Borenstein AR The burden of neurological disease in the United States: A summary report and call to action. Ann. Neurol 81, 479–484 (2017). [PubMed: 28198092]
2. Rajasethupathy P, Ferenczi E & Deisseroth K Targeting Neural Circuits. Cell 165, 524–534 (2016). [PubMed: 27104976]
3. Nordhausen CT, Maynard EM & Normann RA Single unit recording capabilities of a 100 microelectrode array. Brain Research 726, 129–140 (Elsevier, 1996). [PubMed: 8836553]
4. Campbell PK, Jones KE, Huber RJ, Horch KW & Normann RA A silicon-based, three-dimensional neural interface: manufacturing processes for an intracortical electrode array. IEEE Trans. Biomed. Eng 38, 758–768 (1991). [PubMed: 1937509]
5. Jun JJ et al. Fully integrated silicon probes for high-density recording of neural activity. Nature 551, 232–236 (2017). [PubMed: 29120427]
6. Ward MP, Rajdev P, Ellison C & Irazoqui PP Toward a comparison of microelectrodes for acute and chronic recordings. Brain Res. 1282, 183–200 (2009). [PubMed: 19486899]
7. Nolta NF, Christensen MB, Crane PD, Skousen JL & Tresco PA BBB leakage, astrogliosis, and tissue loss correlate with silicon microelectrode array recording performance. (2015).
8. Fu TM et al. Stable long-term chronic brain mapping at the single-neuron level. Nat. Methods 13, 875–882 (2016). [PubMed: 27571550]
9. Hong G et al. A method for single-neuron chronic recording from the retina in awake mice.
10. Lu Y, Lyu H, Richardson AG, Lucas TH & Kuzum D Flexible Neural Electrode Array Based-on Porous Graphene for Cortical Microstimulation and Sensing. Sci. Rep 6, 1–9 (2016). [PubMed: 28442746]
11. Tybrandt K et al. High-Density Stretchable Electrode Grids for Chronic Neural Recording. Adv. Mater 30, (2018).
12. Lu C et al. Flexible and stretchable nanowire-coated fibers for optoelectronic probing of spinal cord circuits. Sci. Adv 3, (2017).
13. Choi S et al. Highly conductive, stretchable and biocompatible Ag-Au core-sheath nanowire composite for wearable and implantable bioelectronics. doi:10.1038/s41565-018-0226-8
14. Inal S, Rivnay J, Suiu A-O, Malliaras GG & McCulloch I Conjugated Polymers in Bioelectronics. Acc. Chem. Res 51, 1368–1376 (2018). [PubMed: 29874033]
15. Patel PR et al. Insertion of linear 8.4 μm diameter 16 channel carbon fiber electrode arrays for single unit recordings. J. Neural Eng 12, 046009 (2015). [PubMed: 26035638]
16. Patel PR et al. Chronic in vivo stability assessment of carbon fiber microelectrode arrays. J. Neural Eng 13, 066002 (2016). [PubMed: 27705958]

17. Khodagholy D et al. NeuroGrid: recording action potentials from the surface of the brain. Nat. Neurosci 18, 310–315 (2015). [PubMed: 25531570]
18. Rivnay J et al. Structural control of mixed ionic and electronic transport in conducting polymers. Nat. Commun 7, 11287 (2016). [PubMed: 27090156]
19. Zhou A, Johnson BC & Muller R Toward true closed-loop neuromodulation: artifact-free recording during stimulation. Curr. Opin. Neurobiol 50, 119–127 (2018). [PubMed: 29471216]
20. Zemelman BV, Lee GA, Ng M & Miesenböck G Selective photostimulation of genetically chARGed neurons. Neuron 33, 15–22 (2002). [PubMed: 11779476]
21. Deisseroth K & Hegemann P The form and function of channelrhodopsin. Science. 357, eaan5544 (2017).
22. Liu X et al. Optogenetic stimulation of a hippocampal engram activates fear memory recall. Nature 484, 381–385 (2012). [PubMed: 22441246]
23. Felix-Ortiz AC, Burgos-Robles A, Bhagat ND, Leppla CA & Tye KM Bidirectional modulation of anxiety-related and social behaviors by amygdala projections to the medial prefrontal cortex. Neuroscience 321, 197–209 (2016). [PubMed: 26204817]
24. Adamantidis AR, Zhang F, Aravanis AM, Deisseroth K & De Lecea L Neural substrates of awakening probed with optogenetic control of hypocretin neurons. Nature 450, 420–424 (2007). [PubMed: 17943086]
25. Gradinaru V, Mogri M, Thompson KR, Henderson JM & Deisseroth K Optical deconstruction of parkinsonian neural circuitry. Science. 324, 354–359 (2009). [PubMed: 19299587]
26. Mager T et al. High frequency neural spiking and auditory signaling by ultrafast red-shifted optogenetics. Nat. Commun 9, 1750 (2018). [PubMed: 29717130]
27. Ronzitti E et al. Sub-millisecond optogenetic control of neuronal firing with two-photon holographic photoactivation of Chronos. J. Neurosci 37, 10679–10689 (2017). [PubMed: 28972125]
28. Tkatch T et al. Optogenetic control of mitochondrial metabolism and Ca^{2+} signaling by mitochondria-targeted opsins. Proc. Natl. Acad. Sci 201703623 (2017).
29. El-Gaby M et al. Archaerhodopsin Selectively and Reversibly Silences Synaptic Transmission through Altered pH. Cell Rep. 16, 2259–2268 (2016). [PubMed: 27524609]
30. Grimm C et al. Electrical properties , substrate specificity and optogenetic potential of the engineered light- driven sodium pump eKR2. Sci. Rep 1–12 (2018). [PubMed: 29311619]
31. Wietek J et al. Anion-conducting channelrhodopsins with tuned spectra and modified kinetics engineered for optogenetic manipulation of behavior. Sci. Rep 7, 14957 (2017). [PubMed: 29097684]
32. Chuong AS et al. Noninvasive optical inhibition with a red-shifted microbial rhodopsin. Nat. Neurosci 17, 1123–1129 (2014). [PubMed: 24997763]
33. Rost BR et al. Optogenetic acidification of synaptic vesicles and lysosomes. Nat. Neurosci 18, 1845–1852 (2015). [PubMed: 26551543]
34. Scheib U et al. Rhodopsin-cyclases for photocontrol of cGMP/cAMP and 2.3 Å structure of the adenylyl cyclase domain. Nat. Commun 9, 2046 (2018). [PubMed: 29799525]
35. Pisanello F et al. Dynamic illumination of spatially restricted or large brain volumes via a single tapered optical fiber. Nat. Neurosci 20, 1180–1188 (2017). [PubMed: 28628101]
36. Wu F et al. Monolithically Integrated μLEDs on Silicon Neural Probes for High- Resolution Optogenetic Studies in Behaving Animals. Neuron 88, 1136–1148 (2015). [PubMed: 26627311]
37. Wang J et al. Integrated device for combined optical neuromodulation and electrical recording for chronic *in vivo* applications. J. Neural Eng 9, 016001 (2012). [PubMed: 22156042]
38. Jeong JW et al. Wireless Optofluidic Systems for Programmable In Vivo Pharmacology and Optogenetics. Cell 162, 662–674 (2015). [PubMed: 26189679]
39. Lee J, Ozden I, Song Y-K & Nurmikko AV Transparent intracortical microprobe array for simultaneous spatiotemporal optical stimulation and multichannel electrical recording. Nat. Methods 12, 1157–1162 (2015). [PubMed: 26457862]
40. Park S et al. One-step optogenetics with multifunctional flexible polymer fibers. Nat. Neurosci 20, 612–619 (2017). [PubMed: 28218915]

41. Canales A et al. Multifunctional fibers for simultaneous optical, electrical and chemical interrogation of neural circuits in vivo. Nat. Biotechnol 33, 277–284 (2015). [PubMed: 25599177]
42. Chen R, Canales A & Anikeeva P Neural recording and modulation technologies. Nat. Rev. Mater 2, 16093 (2017). [PubMed: 31448131]
43. Rost BR, Schneider-Warme F, Schmitz D & Hegemann P Optogenetic Tools for Subcellular Applications in Neuroscience. Neuron 96, 572–603 (2017). [PubMed: 29096074]
44. Wang W et al. A light- and calcium-gated transcription factor for imaging and manipulating activated neurons. Nat. Biotechnol 35, 864–871 (2017). [PubMed: 28650461]
45. Lee D, Hyun JH, Jung K, Hannan P & Kwon HB A calcium- and light-gated switch to induce gene expression in activated neurons. Nat. Biotechnol 35, 858–863 (2017). [PubMed: 28650460]
46. Taslimi A et al. Optimized second-generation CRY2-CIB dimerizers and photoactivatable Cre recombinase. Nat. Chem. Biol 12, 425–430 (2016). [PubMed: 27065233]
47. O'Banion CP et al. Design and Profiling of a Subcellular Targeted Optogenetic cAMP-Dependent Protein Kinase. Cell Chem. Biol 25, 100–109.e8 (2018). [PubMed: 29104065]
48. Kim EH, Chin G, Rong G, Poskanzer KE & Clark HA Optical Probes for Neurobiological Sensing and Imaging. Acc. Chem. Res 51, 1023–1032 (2018). [PubMed: 29652127]
49. Allen WE et al. Global Representations of Goal-Directed Behavior in Distinct Cell Types of Mouse Neocortex. Neuron 94, 891–907.e6 (2017). [PubMed: 28521139]
50. Ohkura M et al. Genetically Encoded Green Fluorescent Ca2+ Indicators with Improved Detectability for Neuronal Ca2+ Signals. PLoS One 7, e51286 (2012). [PubMed: 23240011]
51. Dana H et al. Sensitive red protein calcium indicators for imaging neural activity. Elife 5, e12727 (2016). [PubMed: 27011354]
52. Piatkevich KD et al. A robotic multidimensional directed evolution approach applied to fluorescent voltage reporters. Nat. Chem. Biol 14, 352–360 (2018). [PubMed: 29483642]
53. Lou S et al. Genetically Targeted All-Optical Electrophysiology with a Transgenic Cre-Dependent Optopatch Mouse. J. Neurosci 36, 11059–11073 (2016). [PubMed: 27798186]
54. Bolbat A & Schultz C Recent developments of genetically encoded optical sensors for cell biology. Biol. Cell 109, 1–23 (2017). [PubMed: 27628952]
55. Lin MZ & Schnitzer MJ Genetically encoded indicators of neuronal activity. Nat. Neurosci 19, 1142–1153 (2016). [PubMed: 27571193]
56. Marvin JS et al. Stability, affinity and chromatic variants of the glutamate sensor iGluSnFR. bioRxiv 235176 (2017).
57. Patriarchi T et al. Ultrafast neuronal imaging of dopamine dynamics with designed genetically encoded sensors. Science. 360, eaat4422 (2018). [PubMed: 29853555]
58. Sun F et al. A Genetically Encoded Fluorescent Sensor Enables Rapid and Specific Detection of Dopamine in Flies, Fish, and Mice. Cell 174, 481–496.e19 (2018). [PubMed: 30007419]
59. Jing M et al. A genetically encoded fluorescent acetylcholine indicator for in vitro and in vivo studies. Nat. Biotechnol 36, 726–737 (2018). [PubMed: 29985477]
60. Zhang WH et al. Monitoring hippocampal glycine with the computationally designed optical sensor GlyFS. Nat. Chem. Biol 14, 861–869 (2018). [PubMed: 30061718]
61. Flusberg BA et al. High-speed, miniaturized fluorescence microscopy in freely moving mice. Nat. Methods 5, 935–938 (2008). [PubMed: 18836457]
62. Ghosh KK et al. Miniaturized integration of a fluorescence microscope. Nat. Methods 8, 871–878 (2011). [PubMed: 21909102]
63. Zong W et al. Fast high-resolution miniature two-photon microscopy for brain imaging in freely behaving mice. Nat. Methods 14, 713–719 (2017). [PubMed: 28553965]
64. Gunaydin LA et al. Natural neural projection dynamics underlying social behavior. Cell 157, 1535–1551 (2014). [PubMed: 24949967]
65. Kim CK et al. Simultaneous fast measurement of circuit dynamics at multiple sites across the mammalian brain. Nat. Methods 13, 325–328 (2016). [PubMed: 26878381]
66. Marshall JD et al. Cell-Type-Specific Optical Recording of Membrane Voltage Dynamics in Freely Moving Mice. Cell 167, 1650–1662.e15 (2016). [PubMed: 27912066]

67. Turtaev S et al. High-fidelity multimode fibre-based endoscopy for deep-brain in vivo imaging. Light Sci. Appl 7, 92 (2018). [PubMed: 30479758]
68. Lu L et al. Wireless optoelectronic photometers for monitoring neuronal dynamics in the deep brain. Proc. Natl. Acad. Sci 115, E1374–E1383 (2018). [PubMed: 29378934]
69. Anderzhanova E & Wotjak CT Brain microdialysis and its applications in experimental neurochemistry. Cell Tissue Res. 354, 27–39 (2013). [PubMed: 24022232]
70. Robinson DL, Hermans A, Seipel AT & Wightman RM Monitoring rapid chemical communication in the brain. Chemical Reviews 108, 2554–2584 (2008). [PubMed: 18576692]
71. Roberts JG & Sombers LA Fast-Scan Cyclic Voltammetry: Chemical Sensing in the Brain and beyond. Anal. Chem 90, 490–504 (2018). [PubMed: 29182309]
72. Rodeberg NT et al. Construction of Training Sets for Valid Calibration of in Vivo Cyclic Voltammetric Data by Principal Component Analysis. Anal. Chem 87, 11484–11491 (2015). [PubMed: 26477708]
73. Johnson JA, Rodeberg NT & Wightman RM Failure of Standard Training Sets in the Analysis of Fast-Scan Cyclic Voltammetry Data. ACS Chem. Neurosci 7, 349–359 (2016). [PubMed: 26758246]
74. Rodeberg NT, Sandberg SG, Johnson JA, Phillips PEM & Wightman RM Hitchhiker's Guide to Voltammetry: Acute and Chronic Electrodes for in Vivo Fast-Scan Cyclic Voltammetry. ACS Chemical Neuroscience 8, 221–234 (2017). [PubMed: 28127962]
75. Schwerdt HN et al. Long-term dopamine neurochemical monitoring in primates. Proc. Natl. Acad. Sci 114, 13260–13265 (2017). [PubMed: 29158415]
76. Clark JJ et al. Chronic microsensors for longitudinal, subsecond dopamine detection in behaving animals. Nature Methods. 7, 126–129 (2009). [PubMed: 20037591]
77. Hobbs CN, Johnson JA, Verber MD & Mark Wightman R An implantable multimodal sensor for oxygen, neurotransmitters, and electrophysiology during spreading depolarization in the deep brain. Analyst 142, 2912–2920 (2017). [PubMed: 28715004]
78. Hamid AA et al. Mesolimbic dopamine signals the value of work. Nat. Neurosci 19, 117–126 (2015). [PubMed: 26595651]
79. Bennet KE et al. A Diamond-Based Electrode for Detection of Neurochemicals in the Human Brain. Front. Hum. Neurosci 10, 102 (2016). [PubMed: 27014033]
80. Taylor IM et al. Enhanced dopamine detection sensitivity by PEDOT/graphene oxide coating on in vivo carbon fiber electrodes. Biosens. Bioelectron 89, 400–410 (2017). [PubMed: 27268013]
81. Wilson LR, Panda S, Schmidt AC & Sombers LA Selective and Mechanically Robust Sensors for Electrochemical Measurements of Real-Time Hydrogen Peroxide Dynamics in Vivo. Anal. Chem 90, 888–895 (2018). [PubMed: 29191006]
82. Smith SK et al. Simultaneous Voltammetric Measurements of Glucose and Dopamine Demonstrate the Coupling of Glucose Availability with Increased Metabolic Demand in the Rat Striatum. ACS Chem. Neurosci 15, 272–280 (2016).
83. Lugo-Morales LZ et al. Enzyme-Modified Carbon-Fiber Microelectrode for the Quantification of Dynamic Fluctuations of Nonelectroactive Analytes Using Fast-Scan Cyclic Voltammetry. Anal. Chem 85, 8780–8786 (2013). [PubMed: 23919631]
84. Burmeister JJ, Palmer M & Gerhardt GA l-lactate measures in brain tissue with ceramic-based multisite microelectrodes. Biosens. Bioelectron 20, 1772–1779 (2005). [PubMed: 15681193]
85. Burmeister JJ et al. Ceramic-based multisite microelectrode arrays for simultaneous measures of choline and acetylcholine in CNS. Biosens. Bioelectron 23, 1382–1389 (2008). [PubMed: 18243683]
86. Day BK, Pomerleau F, Burmeister JJ, Huettl P & Gerhardt GA Microelectrode array studies of basal and potassium-evoked release of l-glutamate in the anesthetized rat brain. J. Neurochem 96, 1626–1635 (2006). [PubMed: 16441510]
87. Ngernsutivorakul T, White TS & Kennedy RT Microfabricated Probes for Studying Brain Chemistry: A Review. ChemPhysChem 1128–1142 (2018). [PubMed: 29405568]
88. Zestos AG & Kennedy RT Microdialysis Coupled with LC-MS/MS for In Vivo Neurochemical Monitoring. AAPS J. 19, 1284–1293 (2017). [PubMed: 28660399]

89. Wong J-MT et al. Benzoyl chloride derivatization with liquid chromatography-mass spectrometry for targeted metabolomics of neurochemicals in biological samples. J. Chromatogr. A 1446, 78–90 (2016). [PubMed: 27083258]

90. Rogers ML et al. Simultaneous monitoring of potassium, glucose and lactate during spreading depolarization in the injured human brain - Proof of principle of a novel real-time neurochemical analysis system, continuous online microdialysis. J. Cereb. Blood Flow Metab 37, 1883–1895 (2017). [PubMed: 27798268]

91. Papadimitriou KI et al. High-Performance Bioinstrumentation for Real-Time Neuroelectrochemical Traumatic Brain Injury Monitoring. Front. Hum. Neurosci 10, 212 (2016). [PubMed: 27242477]

92. Wang M, Roman GT, Schultz K, Jennings C & Kennedy RT Improved Temporal Resolution for in Vivo Microdialysis by Using Segmented Flow. Anal. Chem 80, 5607–5615 (2008). [PubMed: 18547059]

93. Lee WH et al. Microfabrication and in Vivo Performance of a Microdialysis Probe with Embedded Membrane. Anal. Chem 88, 1230–1237 (2016). [PubMed: 26727611]

94. Quiroz C et al. Local Control of Extracellular Dopamine Levels in the Medial Nucleus Accumbens by a Glutamatergic Projection from the Infralimbic Cortex. J. Neurosci 36, 851–859 (2016). [PubMed: 26791215]

95. Al-Hasani R et al. In vivo detection of optically-evoked opioid peptide release. Elife 7, e36520 (2018). [PubMed: 30175957]

96. Alexander GM et al. Remote Control of Neuronal Activity in Transgenic Mice Expressing Evolved G Protein-Coupled Receptors. Neuron 63, 27–39 (2009). [PubMed: 19607790]

97. Vardy E et al. A New DREADD Facilitates the Multiplexed Chemogenetic Interrogation of Behavior. Neuron 86, 936–946 (2015). [PubMed: 25937170]

98. Hüll K, Morstein J & Trauner D In Vivo Photopharmacology. Chem. Rev 118, 10710–10747 (2018). [PubMed: 29985590]

99. Broichhagen J, Frank JA & Trauner D A Roadmap to Success in Photopharmacology. Acc. Chem. Res 48, 1947–1960 (2015). [PubMed: 26103428]

100. Banala S et al. Photoactivatable drugs for nicotinic optopharmacology. Nat. Methods 15, 347–350 (2018). [PubMed: 29578537]

101. Dong M, Babalhavaeji A, Samanta S, Beharry AA & Woolley GA Red-Shifting Azobenzene Photoswitches for in Vivo Use. Acc. Chem. Res 48, 2662–2670 (2015). [PubMed: 26415024]

102. Wagner N, Stephan M, Höglinger D & Nadler A A click cage: Organelle-specific uncaging of lipid messengers. Angew. Chemie Int. Ed 57, 13339–13343 (2018).

103. Nadler A et al. Exclusive photorelease of signalling lipids at the plasma membrane. Nat. Commun 6, 10056 (2015). [PubMed: 26686736]

104. Yang G et al. Genetic targeting of chemical indicators in vivo. Nat. Methods 12, 137–139 (2015). [PubMed: 25486061]

105. Shields BC et al. Deconstructing behavioral neuropharmacology with cellular specificity. Science. 356, eaaj1682 (2017).

106. Berry MH et al. Restoration of patterned vision with an engineered photoactivatable G protein-coupled receptor. Nat. Commun 8, 1682 (2017). [PubMed: 29167452]

107. Levitz J et al. Dual optical control and mechanistic insights into photoswitchable group II and III metabotropic glutamate receptors. Proc. Natl. Acad. Sci 114, E3546–E3554 (2017). [PubMed: 28396447]

108. Takemoto K et al. Optical inactivation of synaptic AMPA receptors erases fear memory. Nat. Biotechnol 35, 38–47 (2017). [PubMed: 27918547]

109. Tischbirek C, Birkner A, Jia H, Sakmann B & Konnerth A Deep two-photon brain imaging with a red-shifted fluorometric Ca2+ indicator. Proc. Natl. Acad. Sci 112, 11377–11382 (2015). [PubMed: 26305966]

110. Deal PE, Kulkarni RU, Al-Abdullatif SH & Miller EW Isomerically Pure Tetramethylrhodamine Voltage Reporters. J. Am. Chem. Soc 138, 9085–9088 (2016). [PubMed: 27428174]

111. Martineau M et al. Semisynthetic fluorescent pH sensors for imaging exocytosis and endocytosis. Nat. Commun 8, 1412 (2017). [PubMed: 29123102]

112. Sallin O et al. Semisynthetic biosensors for mapping cellular concentrations of nicotinamide adenine dinucleotides. Elife 7, e32638 (2018). [PubMed: 29809136]
113. Shin H et al. Neural probes with multi-drug delivery capability. Lab Chip 15, 3730–3737 (2015). [PubMed: 26235309]
114. Uguz I et al. A Microfluidic Ion Pump for In Vivo Drug Delivery. Adv. Mater 29, 1701217 (2017).
115. Schubert R et al. Virus stamping for targeted single-cell infection in vitro and in vivo. Nat. Biotechnol 36, 81–88 (2018). [PubMed: 29251729]
116. Jackman SL et al. Silk Fibroin Films Facilitate Single-Step Targeted Expression of Optogenetic Proteins. Cell Rep. 22, 3351–3361 (2018). [PubMed: 29562189]
117. Chan KY et al. Engineered AAVs for efficient noninvasive gene delivery to the central and peripheral nervous systems. Nat. Neurosci 20, 1172–1179 (2017). [PubMed: 28671695]
118. Zhao Z et al. Nanoelectronic Coating Enabled Versatile Multifunctional Neural Probes. Nano Lett 17, 4588–4595 (2017). [PubMed: 28682082]
119. Dagdeviren C et al. Miniaturized neural system for chronic, local intracerebral drug delivery. Sci. Transl. Med 10, eaan2742 (2018). [PubMed: 29367347]
120. Jeong J-W et al. Wireless Optofluidic Systems for Programmable In Vivo Pharmacology and Optogenetics. Cell 162, 662–674 (2015). [PubMed: 26189679]
121. Kampasi K et al. Fiberless multicolor neural optoelectrode for in vivo circuit analysis. Sci. Rep 6, 30961 (2016). [PubMed: 27485264]
122. Kampasi K et al. Dual color optogenetic control of neural populations using low-noise, multishank optoelectrodes. Microsystems Nanoeng. 4, 10 (2018).
123. Minev IR et al. Electronic dura mater for long-term multimodal neural interfaces. Science (80-.). 347, 159–163 (2015).
124. Petit-Pierre G, Bertsch A & Renaud P Neural probe combining microelectrodes and a droplet-based microdialysis collection system for high temporal resolution sampling. Lab Chip 16, 917–924 (2016). [PubMed: 26864169]
125. Lee W et al. Transparent, conformable, active multielectrode array using organic electrochemical transistors. Proc. Natl. Acad. Sci 201703886 (2017).
126. Park DW et al. Electrical Neural Stimulation and Simultaneous in Vivo Monitoring with Transparent Graphene Electrode Arrays Implanted in GCaMP6f Mice. ACS Nano 12, 148–157 (2018). [PubMed: 29253337]
127. Thunemann M et al. Deep 2-photon imaging and artifact-free optogenetics through transparent graphene microelectrode arrays. Nat. Commun 9, 2035 (2018). [PubMed: 29789548]
128. Kuzum D et al. Transparent and flexible low noise graphene electrodes for simultaneous electrophysiology and neuroimaging. Nat. Commun 5, 5259 (2014). [PubMed: 25327632]
129. Jiang Y et al. Rational design of silicon structures for optically controlled multiscale biointerfaces. Nat. Biomed. Eng 2, 508–521 (2018). [PubMed: 30906646]
130. Kilias A et al. Optogenetic entrainment of neural oscillations with hybrid fiber probes. J. Neural Eng 15, 056006 (2018). [PubMed: 29923505]
131. Rein M et al. Diode fibres for fabric-based optical communications. Nature 560, 214–218 (2018). [PubMed: 30089921]
132. Qu Y et al. Superelastic Multimaterial Electronic and Photonic Fibers and Devices via Thermal Drawing. Adv. Mater 30, 1707251 (2018).
133. Grena B et al. Thermally-drawn fibers with spatially-selective porous domains. Nat. Commun 8, 364 (2017). [PubMed: 28848237]
134. Montgomery KL, Iyer SM, Christensen AJ, Deisseroth K & Delp SL Beyond the brain : Optogenetic control in the spinal cord and peripheral nervous system. Sci. Transl. Med 8, 337rv5 (2016).
135. Kandel Eric R. , Schwartz James H., Jessell Thomas M., Siegelbaum Steven A., Hudspeth AJ, A. J. H. Principles of Neural Science, Fifth Edition (Principles of Neural Science (Kandel)). (2012).
136. Lee D, Hyun JH, Jung K, Hannan P & Kwon HB A calcium- and light-gated switch to induce gene expression in activated neurons. Nat. Biotechnol 35, 858–863 (2017). [PubMed: 28650460]

137. O'Banion CP et al. Design and Profiling of a Subcellular Targeted Optogenetic cAMP-Dependent Protein Kinase. Cell Chem. Biol 25, 100–109.e8 (2018). [PubMed: 29104065]

138. Pomeroy JE, Nguyen HX, Hoffman BD & Bursac N Genetically Encoded Photoactuators and Photosensors for Characterization and Manipulation of Pluripotent Stem Cells. Theranostics 7, 3539–3558 (2017). [PubMed: 28912894]

139. Kim CK et al. Simultaneous fast measurement of circuit dynamics at multiple sites across the mammalian brain. Nat. Methods 13, 325–328 (2016). [PubMed: 26878381]

140. Robinson DL, Hermans A, Seipel AT & Wightman RM Monitoring rapid chemical communication in the brain. Chemical Reviews 108, 2554–2584 (2008). [PubMed: 18576692]

141. Takemoto K et al. Optical inactivation of synaptic AMPA receptors erases fear memory. Nat. Biotechnol 35, 38–47 (2017). [PubMed: 27918547]

142. Sallin O et al. Semisynthetic biosensors for mapping cellular concentrations of nicotinamide adenine dinucleotides. Elife 7, e32638 (2018). [PubMed: 29809136]

143. Zhao Z et al. Nanoelectronic Coating Enabled Versatile Multifunctional Neural Probes. Nano Lett 17, 4588–4595 (2017). [PubMed: 28682082]

144. Shemesh OA et al. Temporally precise single-cell-resolution optogenetics. Nat. Neurosci 20, 1796–1806 (2017). [PubMed: 29184208]

145. Berlin S et al. Photoactivatable genetically encoded calcium indicators for targeted neuronal imaging. Nat. Methods 12, 852–858 (2015). [PubMed: 26167640]

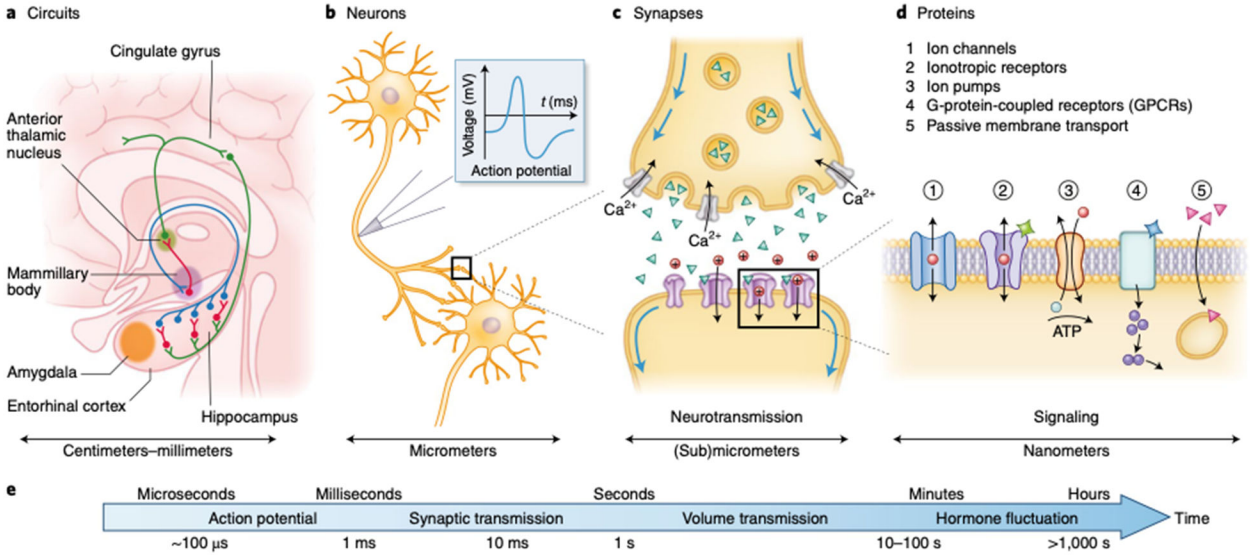

Figure 1. Overview of neuronal communication. A progressively zoomed-in view from a brain circuit to a neuron to a synapse to an ion channel.

(a) Example of a circuit spanning areas across the brain. The Papez circuit involved with emotion and declarative memory. **(b)** Neurons communicate via chemical and electrical signals. Action potential propagates to the synapse, where chemical neurotransmission takes place. **(c)** The presynaptic neuron (top) releases neurotransmitters that diffuse in the synaptic cleft and bind to receptor proteins on the postsynaptic cell (bottom). **(d)** Diversity of membrane receptors in neurons involved in neurotransmission. **(e)** Neuronal communication spans timescales ranging from sub-milliseconds to hours.[135]

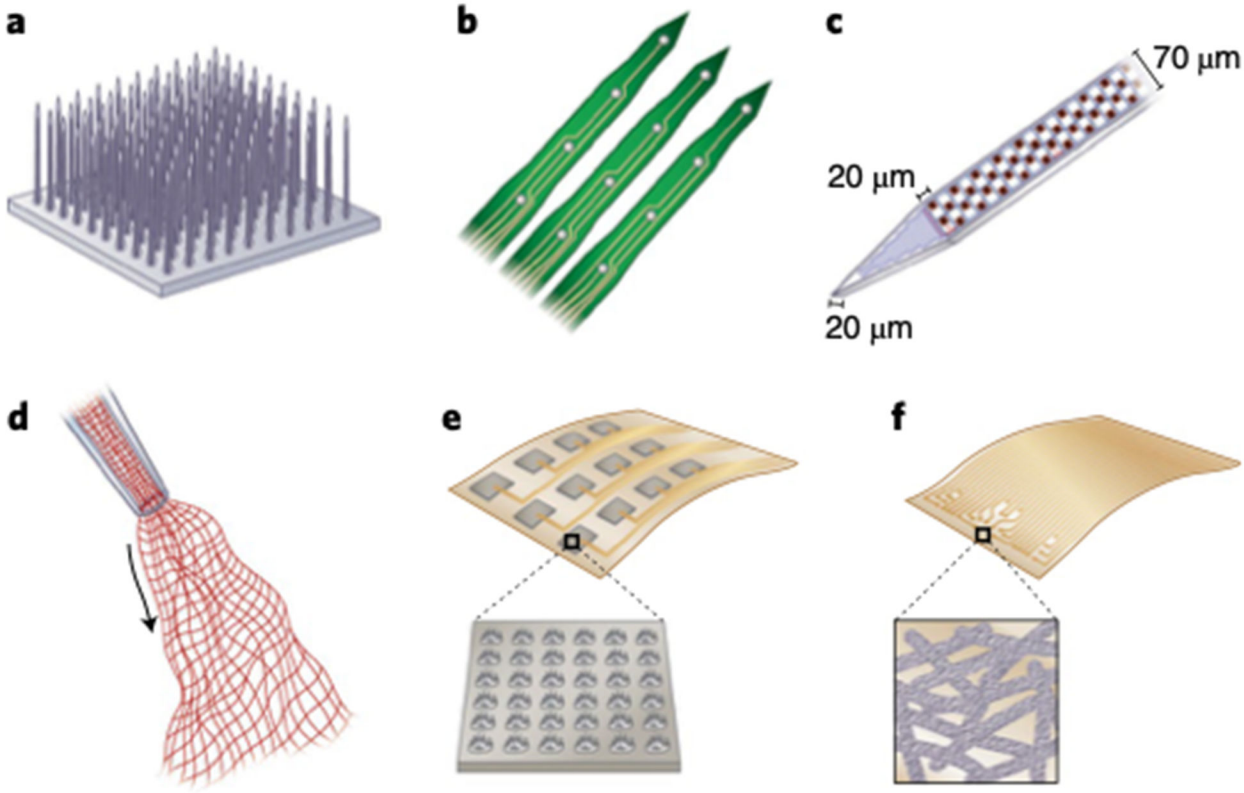

Figure 2. Probes for electrical stimulation and recording of neural activity.

Miocrofabricated silicon-based (**a**) Utah arrays[3] and (**b**) Michigan probes[4]. **(c)** Based on CMOS fabrication process, the Neuropixel features extreme miniaturization and dense packing of 960 recording electrode.[5] **(d)** Syringe injectable mesh electronics based on gold, platinum and SU-8 integrate with the brain and record and stimulate neighboring neurons.[8,9] **(e,f)** Examples of mesh-based electrode arrays: (e) porous graphene electrode on SU-8 substrates[10] and (f) soft and stretchable electrode grids made of Au-TiO_2 nanowires embedded in PDMS[11].

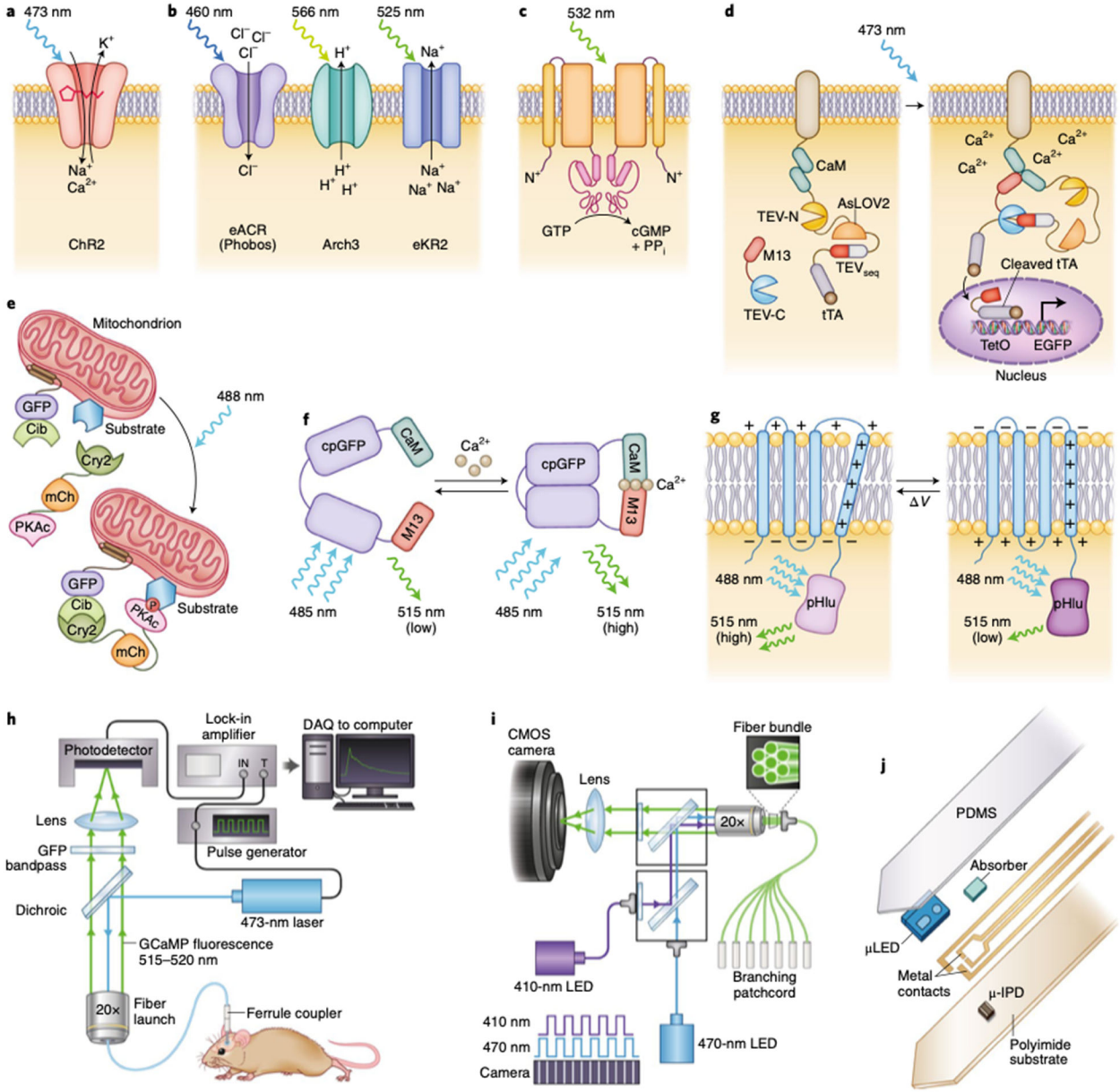

Figure 3. Optical neural stimulation and recording via genetic or non-genetic tools; sensitivity, orthogonality, requirements for hardware.

(a) ChR2 is a cation channel that mediates membrane depolarization upon exposure to blue light. **(b)** Recently developed inhibitory opsins, anion-conducting channelrhodopsin (eACR), proton pump Archaerhodopsin (Arch3.0) and enhanced sodium pump KR2 (eKR2). **(c)** Rhodopsin-guanylyl cyclase chimeric protein CaRhGC consists of a photo-sensitive rhodopsin directly connected to the guanylyl cyclase via a coiled-coil stretch converts GTP to cGMP upon green light illumination[34]. **(d)** In the Cal-Light approach, increase of Ca^{2+} in the cytosol M13 moiety to bind to calmodulin Ca^{2+}-binding domain (CaM), which restores tobacco etch virus (TEV) protease function. LOV-domain photoactivation unmasks TEVseq cleavage site which then releases cleaved tTA to translocate to the nucleus of the cell where it initiates gene expression.[136] **(e)** Light-triggered transfer of an optogenetic cAMP-

dependent protein kinase (OptoPKA) from the cytoplasm to the mitochondria.[137] **(f)** GECI consist of Ca^{2+}-binding CaM, an M13 moiety, and a fluorescent protein. In GCaMP6, binding of Ca^{2+} induces the formation of CaM–M13 complex, which protects the fluorescent core and increases its quantum yield.[138] **(g)** GEVI consists of a voltage-dependent domain and a fluorescent protein. Arclight consist of a voltage-sensing domain fused to super ecliptic pHluorin reporter. Depolarization causes conformation change, which yields a decrease of green fluorescence.[138] **(h)** Single-fiber[64] and **(i)** multi-fiber photometry[139]. Optical fibers transmit excitation light and collect light emitted from GECIs. **(j)** Micro-photometry system for deep-brain fluorescence recording integrating μLEDs and integrated photodetectors (IPDs) encapsulated by PDMS on a polyimide substrate.[68]

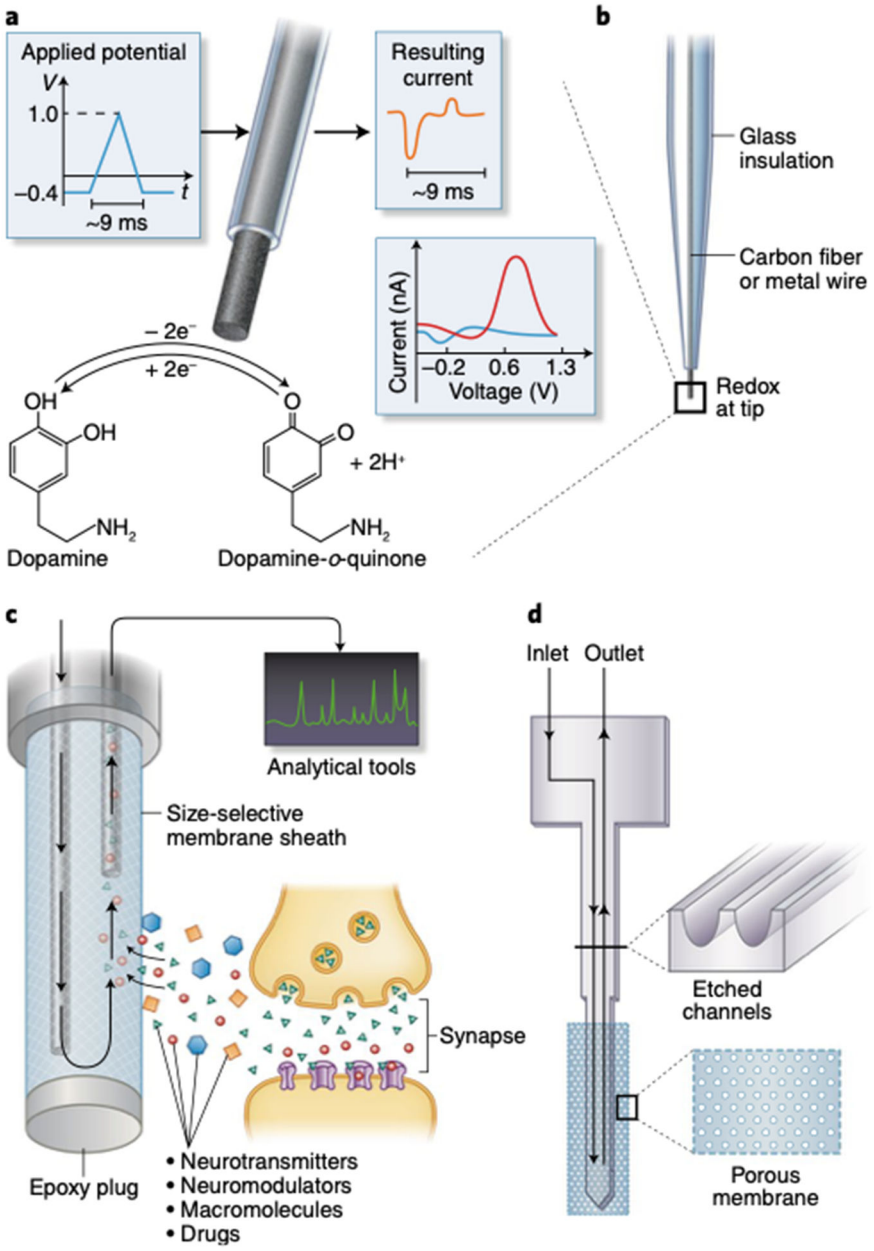

Figure 4. Chemical sensing with voltammetry and microdialysis.

(a) Fast-scan cyclic voltammetry (FSCV) recording of dopamine concentration. Upon application of a triangle potential to the carbon fiber microelectrode, dopamine oxidizes into dopamine-o-quinone and then gets reduced back into dopamine. These electrochemical reactions contribute to the resulting current and form the basis of cyclic voltammogram readout.[140] **(b)** Traditional FSCV probes are made of a carbon fiber or metal wire housed within borosilicate or fused-silica insulating sheaths. The redox reaction occurs at the exposed electrode tip.[87] **(c)** A microdialysis probe is composed of inlet and outlet capillaries housed within a hollow fiber shaft sealed by a size selective membrane sheath infused with buffer. During microdialysis, chemical species diffuse into the hollow cavity and are collected for post-hoc chemical analyses.[87] **(d)** A microfabricated silicon-based

microdialysis probe consists of a U-shaped microfluidic channel with a nanoporous membrane at the tip.[93]

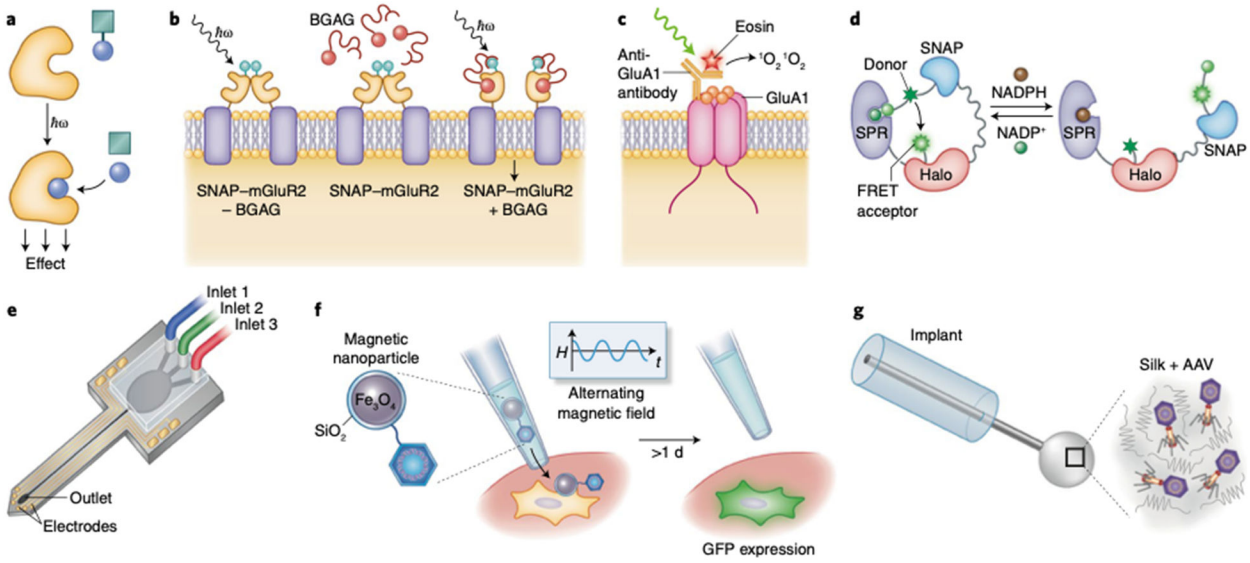

Figure 5. Technologies for chemical modulation and delivery.

(a) A protective group (the cage) is cleaved upon illumination and the ligand becomes biologically active[98]. **(b)** mGluR2 receptor modified to include a SNAP tag is optically controlled via a tethered photoswitchable glutamate BGAG[106]. **(c)** Schematic representation of chromophore-assisted light inactivation (CALI). An anti-GluA1 monoclonal antibody is labeled with eosin, a photosensitizer. Photoactivation by green light and binding of the conjugated antibody to a GluA1 inactivates the targeted receptor containing GluA1[141]. **(d)** A semi-synthetic biosensor NADP-snifit measures NADPH/NADP+ levels via fluorescence shifts in a FRET-pair tethered to a ligand binding domain by Halo and SNAP-tags[142]. **(e)** Schematic representation of the Chemtrode, a microfabricated probe integrating a microelectrode array with a microfluidic channel connected to three separate inlets[113]. **(f)** A GFP-gene carrying virus is reversibly bound to a magnetic nanoparticle that is brought into physical contact with the target cell using magnetic forces and then released upon application of an alternating magnetic field,[115] **(g)** Coating of silk fibroin mixed with adeno-associated virus (AAV) capsids for widespread virus expression in the vicinity of the device.[116]

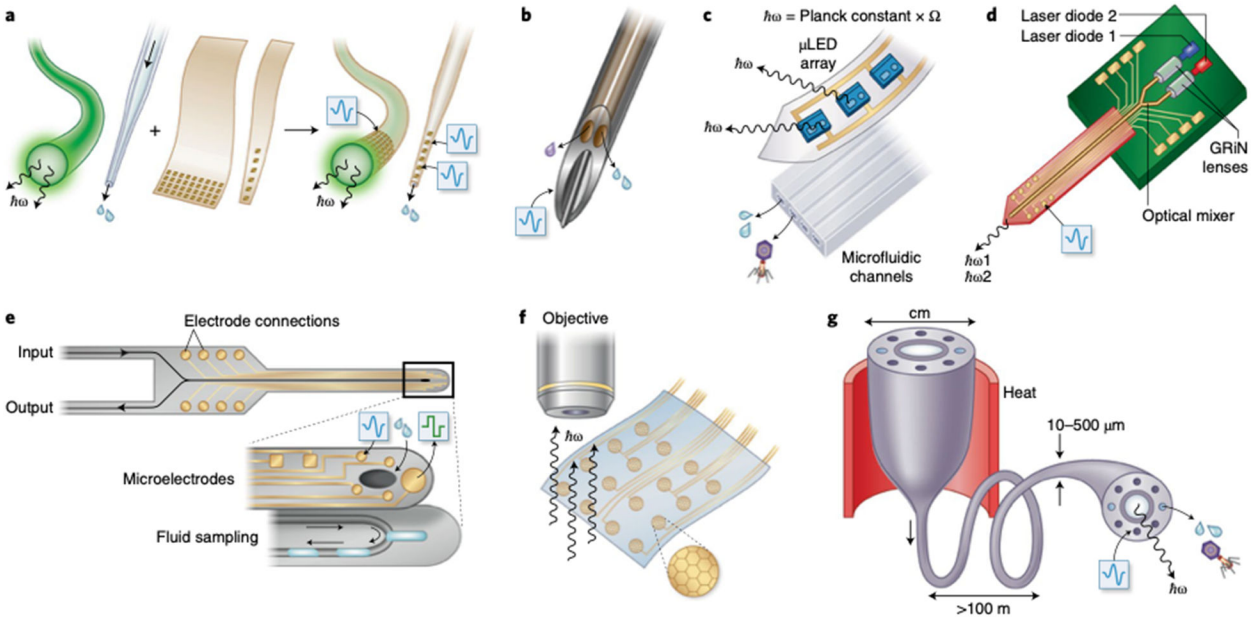

Figure 6. Multimodal integration.

(a) Adhesion of a nanoelectronic coating onto an optical fiber or a micropipette results in bi-modal probes[143]. **(b)** The miniaturized neural drug delivery system (MiNDS) consists of 2 borosilicate microfluidic channels and a tungsten recording electrode inserted into a stainless steel needle[119]. **(c)** Bonding of μ-iLED array on a polymer substrate to a soft PDMS microfluidic device leads to a flexible optofluidic probe[120]. **(d)** The dual-color optoelectrode fuses monolithically integrates an optical mixer with a Michigan-style probe[122]. **(e)** A bi-modal neural probe monolithically integrates microfluidic channels with recording and stimulation electrodes[124]. **(f)** Transparent graphene electrodes fabricated on a flexible parylene C substrate permit electrophysiological recording concomitant with optical imaging with GEVI and optical coherence tomography[126]. **(g)** Thermal drawing of multimaterial macroscale models, preforms, into kilometers of fibers comprising polymer waveguides, conductive composite or metallic electrodes, and microfluidic channels[12,40,41].

Table 1:

Comparison of using electrical, optical, and chemical manipulation and recording of neuronal activity.

Modality	Spatial resolution	Temporal resolution	Sensitivity	Selectivity
Electrical stimulation	Limited by current spreading and electrode dimensions	Sub-microsecond	Highly tunable	Limited −all cells surrounding probe experience field
Electrical recording	<10 μm	Sub-microsecond	>10 μV	Limited - pharmacology required to determine contributors to current
Optical stimulation	Single cell optical stimulation[144]	Sub-microsecond	Highly tunable by irradiation power, wavelength, etc.	High; only light-sensitive reporters will respond
Optical recording	Single cell[145]	Sub-microsecond; can record single action potentials	Limited by available reporters	High; selective biosensors for neurotransmitters and analytes have been developed
FSCV	>100 μm limited by large devices required	≥100 ms	Can detect electroactive molecules over large concentration range	Moderate; care must be taken to validate electrochemical signatures of recording
Microdialysis	>150 μm limited by large size of probes	Seconds to minutes	Sensitivity towards a large range of analytes	High; defined by high- resolution chemical analytics[89]
Chemical stimulation	Limited by diffusion	Seconds to minutes; dictated by diffusion and metabolism	Moderate; tunable through dose applied	High; can be fine-tuned using synthetic chemistry
Chemical recording	Single-cell[109]	Sub-microsecond[110]	Excellent; can be fine-tuned using synthetic chemistry	High − can be fine-tuned using synthetic chemistry